Channel Prediction for Millimeter Wave MIMO Systems in 3D Propagation Environments

Ramoni. O. Adeogun
Department of Electrical Engineering,
School of Engineering and Built Environment,
University of Cape Town,
Cape Town, South Africa
Email: ramoni.adeogun@uct.ac.za

Paul D. Teal and Pawel A. Dmochowski
School of Engineering and Computer Science
Victoria University of Wellington,
Wellington, New Zealand
Email: [paul.teal,pawel.dmochowski]@vuw.ac.nz

***Abstract*—This paper presents a channel prediction method for MIMO systems operating at millimeter wave (mmWave) frequencies in 3D propagation environments. Based on recent 3D model for mmWave channels, an ESPRIT/Unitary ESPRIT approach is proposed for jointly extracting the azimuth, elevation and Doppler parameters of the channel. The MMSE minimum description length (MMDL) criterion is utilize for proper selection of the number of dominant paths. Temporal extrapolation of the estimated model is then performed to obtain future states of the channel. A closed form expression for the performance bound on the estimation and prediction of 3D multiantenna channels with uniform planar array is also derived. The performance of the method is evaluated via numerical simulations.**

***Index Terms*—millimeter wave radio, channel prediction, wireless propagation, parameter estimation, multipath fading.**

I. Introduction

Millimeter–wave (mmWave) frequencies offers several orders of magnitude bandwidth increase as well as beamforming and multiplexing gains through the use of multielement antenna arrays in cellular systems [1]. These potential performance gains can be fully utilized when accurate knowledge of the channel state information (CSI) is available at both the transmitter and receiver [2]. For example, transmit beamforming requires accurate knowledge of the downlink CSI. In frequency division duplex (FDD) systems, CSI is estimated at the receiver and sent back to the transmitter via a feedback link. In practice, the CSI may become outdated before its actual usage as a result of delays in estimation, processing and feedback. Prediction of the CSI is therefore useful for mitigating performance degradations due to channel aging. In time division duplex (TDD) systems, the uplink and downlink channels are reciprocal enabling the transmitter to use the detected downlink CSI as the uplink CSI in time-invariant channels. In time-varying channels, however, the CSI need to be updated via channel prediction.

Channel prediction for traditional multiple input multiple output (MIMO) channels have received considerable research attention within the last few years. In [3]–[6], non-parametric approaches based on autoregressive modeling are developed for MIMO channels. On the hand, parametric schemes utilizing the spatial and temporal structure of MIMO channels for prediction are presented in [7].

The aforementioned MIMO prediction algorithms consider 2D (azimuth only) propagation with linear antenna arrays. In mmWave, 3D (azimuth and elevation) propagation has been the focus of active research (see e.g., [8], [9] and the references therein). The idea is to utilize the additional degrees of freedom in the elevation spectrum. Since existing MIMO channel prediction algorithms are two dimensional in that they assume wave propagation only in the azimuth spectra, there is the need to develop algorithms which account for the impact of the channel component in the elevation direction.

This paper present the results of investigations on the prediction of 3D MIMO channel at mmWave frequencies. The key contributions of the paper are:

- We propose a reduced complexity extension of algorithms for 2D MIMO channel for prediction of 3D channels. The proposed scheme extract the azimuth and elevation spatial parameters as well as the Doppler frequencies from noisy channel estimates using multidimensional unitary ESPRIT (UESPRIT) [10], [11]. Unlike previous schemes, the proposed method considers Uniform Planar Arrays (UPA) at both the transmit and receive end of the system. UPA are of interest in applications such as mmWave beamforming because they enable packing of more antenna elements in reasonably-sized arrays, thereby yielding smaller antenna array dimensions. Moreover, UPAs make beamforming in the elevation domain possible.
- We derive a closed for expression for the performance bound (in the asymptotic limit of large number of samples and/or array sizes) on the prediction of 3D MIMO channels with UPA at both ends.
- We present results on mmWave channel prediction performances using different array geometry.
- A framework for the application of the prediction algorithm to both TDD and FDD system is also presented.

II. Channel Model

We consider a 3D mmWave MIMO channel model defined as [9]

$$\mathbf{H}(t) = \frac{1}{L}\sum_{\ell=1}^{L}\sum_{p=1}^{P_\ell}\alpha_{\ell p}\mathbf{a}_{\mathrm{r}}(\mu^{\mathrm{r}}_{\ell p},\nu^{\mathrm{r}}_{\ell p})\mathbf{a}^T_{\mathrm{t}}(\mu^{\mathrm{t}}_{\ell p},\nu^{\mathrm{t}}_{\ell p})e^{j\omega_{\ell p}} \quad (1)$$

where $[\cdot]^T$ denotes non-conjugate transpose, $\alpha_{\ell p}$ and $\omega_{\ell p}$ are the complex amplitude and Doppler shift of the pth ray in the ℓth cluster. $\mu^{\mathrm{r}}_{\ell p}(\nu^{\mathrm{r}}_{\ell p})$ and $\mu^{\mathrm{t}}_{\ell p}(\nu^{\mathrm{t}}_{\ell p})$ are the azimuth (elevation) spatial directions of arrival and departure, respectively. The vectors $\mathbf{a}_{\mathrm{r}}(\mu^{\mathrm{r}}_{\ell p},\nu^{\mathrm{r}}_{\ell p})$ and $\mathbf{a}_{\mathrm{t}}(\mu^{\mathrm{t}}_{\ell p},\nu^{\mathrm{t}}_{\ell p})$ are the receive and transmit array steering vectors.Assuming that the channel is sampled at interval T_{samp} and combining indices in (1), we obtain

$$\mathbf{H}(k) = \sum_{z=1}^{Z}\beta_z\mathbf{a}_{\mathrm{r}}(\mu^{\mathrm{r}}_{z},\nu^{\mathrm{r}}_{z})\mathbf{a}^T_{\mathrm{t}}(\mu^{\mathrm{t}}_{z},\nu^{\mathrm{t}}_{z})e^{jk\eta_z} \quad (2)$$

where k is the sample index, $\eta_z = T_{\mathrm{samp}}\omega_z$ is the normalized Doppler frequency and $Z = \sum_{\ell=1}^{L}P_\ell$ is the total number of propagating rays. Each ray is characterized by the parameter set $\{\beta_z, \mu^{\mathrm{r}}_z, \nu^{\mathrm{r}}_z, \mu^{\mathrm{t}}_z, \nu^{\mathrm{t}}_z, \eta_z\}$. We assume that no two rays share a common parameter set, but different rays may have one or more equal parameters. Note that (2) is valid for all array geometries. We consider a channel with an $N_1 \times N_2$ and $N_3 \times N_4$ UPA at the transmitter and receiver, respectively. For a $N \times M$ UPA, the array response vector is defined as[1]

$$\mathbf{a}(\mu_z,\nu_z) = \left[1,\cdots,e^{j(n\mu_z+m\nu_z)},\cdots,e^{j((N-1)\mu_z+(M-1)\nu_z)}\right] \quad (3)$$

where $0 \le n < N$ and $0 \le m < M$ are the indices of the antenna elements. We assume that K samples of the channel are known from estimation and denote the estimates as

$$\hat{\mathbf{H}}(k) = \mathbf{H}(k) + \mathbf{W}(k) \quad (4)$$

where $\mathbf{N}(k)$ is the additive complex Gaussian noise.

III. The Proposed 3D Prediction Method

Given the model in (2) and the K samples in (4), our aim is to estimate the number of dominant rays $\hat{Z}$ and the parameter set $\{\beta_z, \mu^{\mathrm{r}}_z, \nu^{\mathrm{r}}_z, \mu^{\mathrm{t}}_z, \nu^{\mathrm{t}}_z, \eta_z\}_{z=1}^{\hat{Z}}$ and use (2) to perform time extrapolation of the channel. The procedures required for the prediction are presented in this section.

A. Data Preprocessing

Letting $\hat{\mathbf{h}}(k) = \mathrm{vec}[\hat{\mathbf{H}}(k)]$ be an $N_1N_2N_3N_4 \times 1$ vector obtained by stacking the columns of (4), we form the Hankel matrix

$$\hat{\mathbf{D}} = \begin{bmatrix} \hat{\mathbf{h}}(0) & \hat{\mathbf{h}}(1) & \cdots & \hat{\mathbf{h}}(Q) \\ \hat{\mathbf{h}}(1) & \hat{\mathbf{h}}(2) & \cdots & \hat{\mathbf{h}}(Q+1) \\ \vdots & \vdots & \ddots & \vdots \\ \hat{\mathbf{h}}(R) & \hat{\mathbf{h}}(R+1) & \cdots & \hat{\mathbf{h}}(K-1) \end{bmatrix} \quad (5)$$

where $Q = K - R$. The covariance matrix is then estimated from (5) using

$$\hat{\mathbf{R}} = \hat{\mathbf{D}}\hat{\mathbf{D}}^H/(N_1N_2N_3N_4R) \quad (6)$$

where $[\cdot]^H$ denotes the Hermitian transpose.

B. Joint Parameter Estimation

Using the eigenvalues of $\hat{\mathbf{R}}$, we estimate the number of dominant rays, $\hat{Z}$ using the minimum mean squared error (MMSE)–minimum description length criterion [12]. In order to estimate the parameters $\{\beta_z, \mu^{\mathrm{r}}_z, \nu^{\mathrm{r}}_z, \mu^{\mathrm{t}}_z, \nu^{\mathrm{t}}_z, \eta_z\}_{z=1}^{\hat{Z}}$, we utilize a 5D extension of the Unitary ESPRITapproach[2] [11] . By applying forward backward averaging on (6), we obtain a centro-Hermitian covariance matrix which is coverted into a real-valued matrix, thus

$$\hat{\mathbf{C}} = \frac{1}{2}\left[\mathbf{Q}^H_T\{\hat{\mathbf{R}} + \Pi_T\hat{\mathbf{R}}^*\Pi_T\}\mathbf{Q}_T\right] \quad (7)$$

where * denotes the complex conjugate operation, Π_m is the $m \times m$ exchange matrix with ones on its antidiagonal and zeros elsewhere, and $\mathbf{Q}_m$ is a unitary left-real matrix, defined as

$$\mathbf{Q}_m = \begin{cases} \frac{1}{\sqrt{2}}\begin{bmatrix} \mathbf{I}_k & j\mathbf{I}_k \\ \mathbf{\Pi}_k & -j\mathbf{\Pi}_k \end{bmatrix}, & m = 2k \\ \frac{1}{\sqrt{2}}\begin{bmatrix} \mathbf{I}_k & 0 & j\mathbf{I}_k \\ \mathbf{0}^T_k & \sqrt{2} & \mathbf{0}^T_k \\ \mathbf{\Pi}_k & 0 & -j\mathbf{\Pi}_k \end{bmatrix}, & m = 2k+1 \end{cases} \quad (8)$$

Letting $\mathbf{U}_{\mathrm{s}}$ be the signal subspace matrix having the eigenvectors corresponding to the $\hat{Z}$ largest eigenvalues of $\hat{\mathbf{C}}$ in (7), we form the following invariance equations

$$\mathbf{K}_{i,1}\mathbf{U}_{\mathrm{s}}\mathbf{\Lambda}_1 = \mathbf{K}_{i,2}\mathbf{U}_{\mathrm{s}};\ i = 1,2,\cdots,5 \quad (9)$$

where $\mathbf{K}_{i,j}; j = 1,2$ are transformed selection matrices

$$\begin{aligned} \mathbf{K}_{i,1} &= 2\cdot\mathrm{Re}\{\mathbf{Q}^H_T\mathbf{J}_{i,2}\mathbf{Q}_T\} \\ \mathbf{K}_{i,2} &= 2\cdot\mathrm{Im}\{\mathbf{Q}^H_T\mathbf{J}_{i,2}\mathbf{Q}_T\} \end{aligned} \quad (10)$$

where $\mathrm{Re}\{\cdot\}$ and $\mathrm{Im}\{\cdot\}$ denotes the real and complex part of the associated matrix, respectively. The selection matrices $\mathbf{J}_{i,2}$ are defined as

$$\begin{aligned} \mathbf{J}_{1,2} &= [\mathbf{0}_{N_1-1}\quad \mathbf{I}_{N_1-1}]\otimes\mathbf{I}_{N_2}\otimes\mathbf{I}_{N_3}\otimes\mathbf{I}_{N_4}\otimes\mathbf{I}_R \\ \mathbf{J}_{2,2} &= \mathbf{I}_{N_1}\otimes[\mathbf{0}_{N_2-1}\quad \mathbf{I}_{N_2-1}]\otimes\mathbf{I}_{N_3}\otimes\mathbf{I}_{N_4}\otimes\mathbf{I}_R \\ \mathbf{J}_{3,2} &= \mathbf{I}_{N_1}\otimes\mathbf{I}_{N_2}\otimes[\mathbf{0}_{N_3-1}\quad \mathbf{I}_{N_3-1}]\otimes\mathbf{I}_{N_4}\otimes\mathbf{I}_R \\ \mathbf{J}_{4,2} &= \mathbf{I}_{N_1}\otimes\mathbf{I}_{N_2}\otimes\mathbf{I}_{N_3}\otimes[\mathbf{0}_{N_4-1}\quad \mathbf{I}_{N_4-1}]\otimes\mathbf{I}_R \\ \mathbf{J}_{5,2} &= \mathbf{I}_{N_1}\otimes\mathbf{I}_{N_2}\otimes\mathbf{I}_{N_3}\otimes\mathbf{I}_{N_4}\otimes[\mathbf{0}_{R-1}\quad \mathbf{I}_{R-1}] \end{aligned} \quad (11)$$

After solving the equations in (10) in the least sense, the parameter estimates are obtained using

$$\hat{\boldsymbol{\mu}}^i = 2\cdot\tan^{-1}(\mathrm{diag}[\mathrm{eig}\{\mathbf{\Lambda}_i\}]);\ i = 1,\cdots,5 \quad (12)$$

where $\mathrm{diag}[\cdot]$ and $\mathrm{eig}\{\cdot\}$ represents the diagonal entries and eignevalues of the associated matrix, respectively.

[1]The definition of the spatial directions μ and ν in terms of the azimuth and elevation angles of arrival/departure depends on the array orientation.

[2]The ESPRIT based approaches in [13] can also be extended to 3D propagation following a similar procedure as presented in this Section.

C. Complex Amplitude Estimation

Let $\hat{\mathbf{h}}_{11} = [\hat{h}_{11}(0), \cdots, \hat{h}_{11}(K-1)]^T$ be the K samples of the channel between the first transmit and receive antenna element. Using (2) and the parameter estimates in (12), $\hat{\mathbf{h}}_{11}$ can be expressed as

$$\hat{\mathbf{h}}_{11} = \hat{\mathbf{F}}\boldsymbol{\beta} + \mathbf{w} \tag{13}$$

where $\mathbf{F}$ is the Vandermonde matrix

$$\mathbf{F} = \begin{bmatrix} 1 & \cdots & 1 \\ e^{j\hat{\eta}_1} & \cdots & e^{j\hat{\eta}_{hatZ}} \\ \vdots & \ddots & \vdots \\ e^{j(K-1)\hat{\eta}_1} & \cdots & e^{j(K-1)\hat{\eta}_{hatZ}} \end{bmatrix} \tag{14}$$

By minimizing the miminum mean square error (MMSE) in (13), we obtain

$$\hat{\boldsymbol{\beta}} = (\hat{\mathbf{F}}^H\hat{\mathbf{F}})^{-1}\hat{\mathbf{F}}^H\hat{\mathbf{h}}_{11} \tag{15}$$

IV. 3D Prediction Error Bound

In this section, we derive closed–form expression for the error bound on the prediction of 3D MIMO channels in the asympotic limit of large array sizes and/or number of samples.

A. Prediction Bound

Let the parametrization of the 3D channel be defined as

$$\boldsymbol{\Theta} = \begin{bmatrix} \Re(\boldsymbol{\beta}) & \Im(\boldsymbol{\beta}) & \boldsymbol{\mu}^{\mathrm{r}} & \boldsymbol{\nu}^{\mathrm{r}} & \boldsymbol{\mu}^{\mathrm{t}} & \boldsymbol{\nu}^{\mathrm{t}} & \boldsymbol{\eta} \end{bmatrix} \tag{16}$$

$\Re[\cdot]$ and $\Im[\cdot]$ denote the real and imaginary parts of the associated complex number, respectively. Following similar procedure presented in [14], the prediction error bound can be obtained using

$$\mathrm{MSEB}(k) = \mathrm{Tr}\left[\frac{\partial \mathbf{h}(k)}{\partial \boldsymbol{\Theta}}^H \mathbf{I}^{-1}(\boldsymbol{\Theta})\frac{\partial \mathbf{h}(k)}{\partial \boldsymbol{\Theta}}\right] \tag{17}$$

where

$$\frac{\partial \mathbf{h}}{\partial \Theta} = \mathbf{P}_5 \diamond \mathbf{P}_4 \diamond \mathbf{P}_3 \diamond \mathbf{P}_2 \diamond \mathbf{P}_1 \diamond \mathbf{P}_0 \tag{18}$$

and

$$[\mathbf{I}(\Theta)] = \frac{2}{\sigma^2}\Re\left[(\mathbf{P}_5^H\mathbf{P}_5) \odot (\mathbf{P}_4^H\mathbf{P}_4)\cdots \odot (\mathbf{P}_0^H\mathbf{P}_0)\right] \tag{19}$$

The matrices $\mathbf{P}_0$ –$\mathbf{P}_5$ are obtained for the 3D channel as

$$\mathbf{P}_0 = \begin{bmatrix} \boldsymbol{\beta}^T & \boldsymbol{\beta}^T & \boldsymbol{\beta}^T & \boldsymbol{\beta}^T & \boldsymbol{\beta}^T & \mathbf{1}^1 & j\mathbf{1}^T \end{bmatrix} \tag{20}$$

$$\mathbf{P}_1 = [\mathbf{D}_{\mu}^{\mathrm{r}} \quad \mathbf{A}_{\mu}^{\mathrm{r}} \quad \mathbf{A}_{\mu}^{\mathrm{r}} \quad \mathbf{A}_{\mu}^{\mathrm{r}} \quad \mathbf{A}_{\mu}^{\mathrm{r}} \quad \mathbf{A}_{\mu}^{\mathrm{r}} \quad \mathbf{A}_{\mu}^{\mathrm{r}}] \tag{21}$$

$$\mathbf{P}_2 = [\mathbf{A}_{\nu}^{\mathrm{r}} \quad \mathbf{D}_{\nu}^{\mathrm{r}} \quad \mathbf{A}_{\nu}^{\mathrm{r}} \quad \mathbf{A}_{\nu}^{\mathrm{r}} \quad \mathbf{A}_{\nu}^{\mathrm{r}} \quad \mathbf{A}_{\nu}^{\mathrm{r}} \quad \mathbf{A}_{\nu}^{\mathrm{r}}] \tag{22}$$

$$\mathbf{P}_3 = [\mathbf{A}_{\mu}^{\mathrm{t}} \quad \mathbf{A}_{\mu}^{\mathrm{t}} \quad \mathbf{D}_{\mu}^{\mathrm{t}} \quad \mathbf{A}_{\mu}^{\mathrm{t}} \quad \mathbf{A}_{\mu}^{\mathrm{t}} \quad \mathbf{A}_{\mu}^{\mathrm{t}} \quad \mathbf{A}_{\mu}^{\mathrm{t}}] \tag{23}$$

$$\mathbf{P}_4 = [\mathbf{A}_{\nu}^{\mathrm{t}} \quad \mathbf{A}_{\nu}^{\mathrm{t}} \quad \mathbf{A}_{\nu}^{\mathrm{t}} \quad \mathbf{D}_{\nu}^{\mathrm{t}} \quad \mathbf{A}_{\nu}^{\mathrm{t}} \quad \mathbf{A}_{\nu}^{\mathrm{t}} \quad \mathbf{A}_{\nu}^{\mathrm{t}}] \tag{24}$$

$$\mathbf{P}_5 = [\mathbf{A}_{\eta} \quad \mathbf{A}_{\eta} \quad \mathbf{A}_{\eta} \quad \mathbf{A}_{\eta} \quad \mathbf{D}_{\eta} \quad \mathbf{A}_{\eta} \quad \mathbf{A}_{\eta}] \tag{25}$$

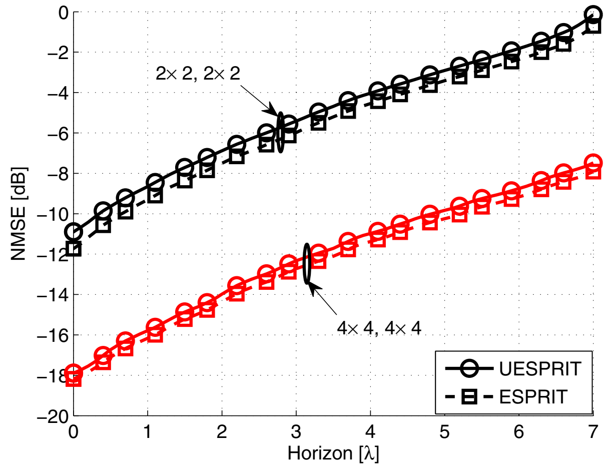

Fig. 1. Normalized Mean Squared Prediction Error versus horizon for both UESPRIT and ESPRIT based approaches. UPA with different array sizes are considered.

B. Asymptotic Bound

Following similar procedure presented in [14], the Fisher Information Matrix (FIM) for the zth path is obtained as

$$\mathfrak{J}_z = a\begin{bmatrix} 2 & 0 & 0 & 0 & 0 & 0 & 0 \\ 0 & 2 & 0 & 0 & 0 & 0 & 0 \\ 0 & 0 & \frac{2N_1^2}{3} & \frac{N_1N_2}{2} & \frac{N_1N_3}{2} & \frac{N_1N_4}{2} & \frac{N_1K}{2} \\ 0 & 0 & \frac{N_1N_2}{2} & \frac{2N_2^2}{3} & \frac{N_2N_3}{2} & \frac{N_2N_4}{2} & \frac{N_2K}{2} \\ 0 & 0 & \frac{N_1N_3}{2} & \frac{N_2N_3}{2} & \frac{2N_3^2}{3} & \frac{N_3N_4}{2} & \frac{N_3K}{2} \\ 0 & 0 & \frac{N_1N_4}{2} & \frac{N_2N_4}{2} & \frac{N_3N_4}{2} & \frac{2N_4^2}{3} & \frac{N_4K}{2} \\ 0 & 0 & \frac{N_1K}{2} & \frac{N_2K}{2} & \frac{N_3K}{2} & \frac{N_4K}{2} & \frac{2K^2}{3} \end{bmatrix} \tag{26}$$

where $a = N_1N_2N_3N_4K/\sigma^2$. On inverting (26), we obtain the asymptotic bound on the parameter estimates covariance as

$$\mathfrak{F}_z = \frac{1}{a}\begin{bmatrix} \frac{1}{2} & 0 & 0 & 0 & 0 & 0 & 0 \\ 0 & \frac{1}{2} & 0 & 0 & 0 & 0 & 0 \\ 0 & 0 & \frac{39}{8N_1^2} & \frac{-9}{8N_1N_2} & \frac{-9}{8N_1N_3} & \frac{-9}{8N_1N_4} & \frac{9}{8N_1K} \\ 0 & 0 & \frac{-9}{8N_1N_2} & \frac{39}{8N_2^2} & \frac{-9}{8N_2N_3} & \frac{-9}{8N_2N_4} & \frac{9}{8N_2K} \\ 0 & 0 & \frac{-9}{8N_1N_3} & \frac{-9}{8N_2N_3} & \frac{39}{8N_3^2} & \frac{-9}{8N_3N_4} & \frac{9}{8N_3K} \\ 0 & 0 & \frac{-9}{8N_1N_4} & \frac{-9}{8N_2N_4} & \frac{-9}{8N_3N_4} & \frac{39}{8N_4^2} & \frac{9}{8N_4K} \\ 0 & 0 & \frac{9}{8N_1K} & \frac{9}{8N_2K} & \frac{9}{8N_3K} & \frac{9}{8N_4K} & \frac{39}{8K^2} \end{bmatrix} \tag{27}$$

Similarly, the asymptotic normalized mean square error bound (ANMSEB) is obtained as

$$\mathrm{ANMSEB}(k) = \frac{Z\sigma^2}{8N_1N_2N_3N_4K}\left[33 - \frac{36k}{K} + \frac{39k^2}{K^2}\right] \tag{28}$$

V. Numerical Simulations

In this section, we evaluate the performance of the proposed prediction scheme and compare with the derived asymptotic error bound. We consider a mmWave MIMO channel with

TABLE I
SUMMARY OF MMWAVE AND MCWAVE NLOS LARGE SCALE AND SMALL SCALE PARAMETERS

Variable	Model Parameter Values		
	mcWave	28 GHz	73 GHz
Omni. path loss, PL	Scen. Dependent	$\alpha = 72,\ \beta = 2.92$	$\alpha = 86.6,\ \beta = 2.45$
Number of Clusters, K	8 – 20	$\lambda = 1.8$	$\lambda = 1.9$
Horizontal cluster central angles	$\theta, \phi \sim \mathbf{N}(30.8, 12.5)$	$\theta, \phi \sim \mathbf{U}(0, 2\pi)$	
Vertical cluster central angles	$\vartheta, \varphi \sim \mathbf{N}(66.9, 15.1)$	$\vartheta, \varphi \sim=$ LOS elevation angle	
AOA/AOD	Wrapped Gaussian	Wrapped Gaussian around central angles	

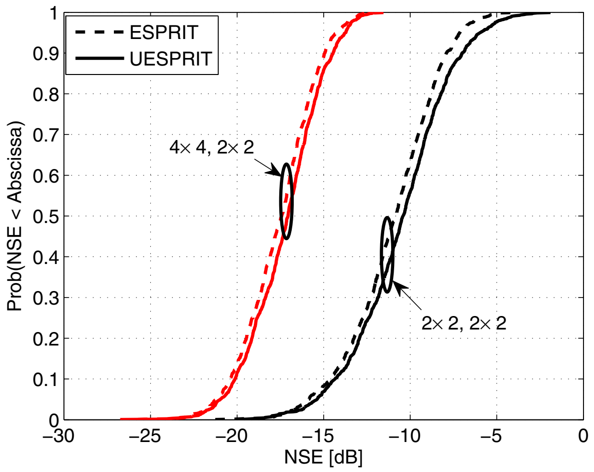

Fig. 2. CDF of prediction error as a function of SNR for a prediction horizon of $1\,\lambda$.

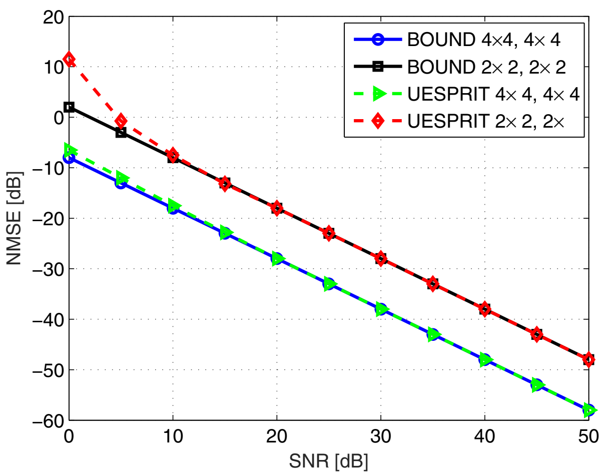

Fig. 3. Comparizon of the performance of proposed UESPRIT based scheme with asymptotic prediction error bound for a mmWave channel.

parameters presented in Table I. We consider a MIMO system with UPA at both ends of the link. The inter-element distance of the array is chosen as $1/2\,\lambda$ and the array orientation is assumed to be in the x - z plane. Without loss of generality, we limit the size of the rectangular array to a maximum of 4×4 (equivalent to 16 array elements). The channel is generated randomly using the parameters in Table I and the model in Section II. Except where otherwise stated, a mobile velocity of $50\,Km/h$ is considered in our simulations and results are averaged over 1000 realizations of the channel.

In Figure 1, we compare the performance of the proposed Unitary ESPRIT based prediction approach with classical ESPRIT based method in existing literature. We plot the normalized mean square error (NMSE) versus the prediction length (in wavelengths) at a signal to noise ratio (SNR) of 10 dB. We observe that the prediction performance degrades with increasing prediction horizon for both array sizes considered. No significant difference is observed between the reduced complexity method proposed in this paper and the existing ESPRIT based method. It should be noted that although, our scheme show similar performance with ESPRIT approach. The performance is achieved at a significantly lower computational complexity. This is advantageous considering the array geometry for 3D propagation and the large number of array elements in millimeter wave applications. As expected, increasing the array size decreases the NMSE. A plausible explanation for this is that an increase in array size reveals more structure of the channel resulting in improved estimation of the channel parameters and hence, better prediction. Similar observations are made in Figure 2, where we plot the cumulative distribution function (CDF) of the prediction normalized square error (NSE) against the SNR.

Figure 3 compares the performance of the proposed method with the asymptotic error bound derived in Section IV. We plot the NMSE/error bound versus SNR for a prediction horizon of $1\,\lambda$. We observed that the performance of the propose algorithm approaches the error bound with increasing SNR. For instance, while the difference between the bound and prediction error for a system with 2×2 - UPA at both ends is about 9 dB at SNR =0 dB, the difference is only about 2 dB at an SNR of 5 dB.

VI. CONCLUSION

We have developed a reduced complexity method for the prediction of millimeter wave multiple input multiple output (MIMO) wireless channels in this paper. The proposed scheme extract the azimuth and elevation spatial parameters as well as the Doppler frequencies from noisy 3D channel estimates using multidimensional unitary ESPRIT (UESPRIT) . Unlike existing 2D approaches, Uniform Planar Arrays (UPA) are considered at both the transmit and receive end of the system in this paper. An asymptotic closed form expression on the prediction of 3D MIMO channels have also been derived. Our results show that the proposed scheme offer similar performance compared with the classical ESPRIT based approaches and is asymptotically efficient for the SNR ranges considered. Application of the proposed scheme in typical system architectures utilizing both TDD and FDD is the focus of our ongoing research.

REFERENCES

[1] S. Rangan, T. Rappaport, and E. Erkip, "Millimeter-wave cellular wireless networks: Potentials and challenges," *Proceedings of the IEEE*, vol. 102, no. 3, pp. 366–385, 2014.

[2] M. Sandell, H. Vetter, and F. Tosato, "Joint linear and nonlinear precoding in mimo systems," *IEEE Comm. Letters*, vol. 15, no. 12, pp. 1265–1267, dec 2011.

[3] Z. Xu, M. Hofer, and T. Zemen, "A time-variant channel prediction and feedback framework for interference alignment," *IEEE Transactions on Vehicular Technology*, vol. PP, no. 99, pp. 1–1, 2017.

[4] L. Liu, H. Feng, T. Yang, and B. Hu, "Mimo-ofdm wireless channel prediction by exploiting spatial-temporal correlation," *IEEE Tran. on Wireless Comm.*, vol. 13, no. 1, pp. 310–319, Jan 2014.

[5] I. Wong and B. Evans, "Exploiting spatio-temporal correlations in mimo wireless channel prediction," in *IEEE GLOBECOM*, Nov 2006, pp. 1–5.

[6] R. Nagashima, T. Ohtsuki, W. Jiang, Y. Takatori, and T. Nakagawa, "Channel prediction for massive mimo with channel compression based on principal component analysis," in *2016 IEEE 27th Annual International Symposium on Personal, Indoor, and Mobile Radio Communications (PIMRC)*, Sept 2016, pp. 1–6.

[7] R. Adeogun, P. Teal, and P. Dmochowski, "Parametric channel prediction for narrowband mobile mimo systems using spatio-temporal correlation analysis," in *IEEE 78th VTC (Fall)*, Sept 2013, pp. 1–5.

[8] T. Rappaport, S. Sun, R. Mayzus, H. Zhao, Y. Azar, K. Wang, G. Wong, J. Schulz, M. Samimi, and F. Gutierrez, "Millimeter wave mobile communications for 5g cellular: It will work!" *IEEE Access*, vol. 1, pp. 335–349, 2013.

[9] M. Akdeniz, Y. Liu, M. Samimi, S. Sun, S. Rangan, T. Rappaport, and E. Erkip, "Millimeter wave channel modeling and cellular capacity evaluation," *Selected Areas in Communications, IEEE Journal on*, vol. 32, no. 6, pp. 1164–1179, June 2014.

[10] M. Haardt and J. Nossek, "Unitary esprit: how to obtain increased estimation accuracy with a reduced computational burden," *IEEE Trans. on Sig. Proc.*, vol. 43, no. 5, pp. 1232–1242, May 1995.

[11] F. Roemer and M. Haardt, "Multidimensional Unitary Tensor-ESPRIT for non-circular sources," in *IEEE ICASSP*, April 2009, pp. 3577–3580.

[12] L. Huang, T. Long, E. Mao, H. C. So, and S. Member, "MMSE-Based MDL Method for Accurate Source Number Estimation," *IEEE Sig. Proc.Letters*, vol. 16, no. 9, pp. 798–801, 2009.

[13] R. Adeogun, P. Teal, and P. Dmochowski, "Extrapolation of mimo mobile-to-mobile wireless channels using parametric-model-based prediction," *IEEE Tran. on Vehicular Tech.*, vol. 64, no. 10, pp. 4487–4498, Oct 2015.

[14] R. Adeogun, P. Dmochowski, and P. Teal, "Asymptotic error bounds on prediction of narrowband mimo wireless channels," *IEEE Sig. Proc. Letters*, vol. 21, no. 9, pp. 1103–1107, Sept 2014.